IEEE Access
Multidisciplinary | Rapid Review | Open Access Journal

Received 8 August 2022, accepted 28 August 2022, date of publication 5 September 2022, date of current version 12 September 2022.

Digital Object Identifier 10.1109/ACCESS.2022.3204059

RESEARCH ARTICLE

Extended State Observer Based Integral Sliding Mode Control for Maglev System With Fixed Time Convergence

ATUL SHARMA[1], (Student Member, IEEE), ABDULRAHMAN ALTURKI[2], AND SYED MUHAMMAD AMRR[1], (Graduate Student Member, IEEE)

[1]Department of Electrical Engineering, Indian Institute of Technology Delhi, New Delhi 110016, India
[2]Electrical Engineering Department, College of Engineering, Qassim University, Buraydah 51452, Saudi Arabia

Corresponding author: Syed Muhammad Amrr (syedamrr@gmail.com)

ABSTRACT The purpose of this study is to explore the design of a robust control strategy for regulating the magnetic levitation system, which is affected by model uncertainty and surrounding disturbance. This paper integrates a fixed-time extended state observer (ESO) with a fixed-time integral sliding mode control (ISMC) design. The fixed-time ESO is employed to estimate the total disturbance within the system in a fixed time. The estimated output is then fed to the composite control law to cancel the actual disturbance in the system. Consequently, it avoids large gain for switching function in the ISMC law, thus suppressing the chattering from the control input. It also avoids employing a conservative condition on the advance information of disturbance bound. In addition, the proposed ISMC design ensures fixed time convergence of closed-loop signals. Moreover, since the integral sliding surface has no reaching phase; therefore the proposed composite scheme has a better invariance behavior from the initial time. The Lyapunov stability theory proves the fixed time stability of sliding variable and relative states. Furthermore, the effectiveness of the presented methodology is validated using numerical analysis with a comparative performance of state-of-the-art control schemes. The numerical results of these schemes are judged based on convergence time, residual bound, energy consumption, and total input variation.

INDEX TERMS Extended state observer, Maglev system, integral sliding mode control, fixed time convergence.

I. INTRODUCTION

The concept of magnetic levitation is employed in a wide range of fields. From simple laboratory setups for benchmark problems to huge magnetic levitation (maglev) vehicles like high-speed train transportation. Maglev vehicles operate on the notion of contactless mobility, which has made them a popular mode of transit [1]. The maglev system has also been explored in the research field to study the control of the maglev-based wind turbines [2], high-speed maglev train [3], active magnetic bearings [4], etc. In the engineering sector, maglev technology is a burning topic of research. As the population in metropolitan cities is increasing rapidly, demand for faster and more efficient public transportation has also increased. Hence, the transportation systems need to be more rapid, dependable, and safe to benefit the public while coping with the new generational challenges. Moreover, these systems need to be user-friendly, low-maintenance, environmental friendly, light-weight, and convenient for transportation of large masses [3]. After 40 years of research in the field of maglev systems around the world, it has gained significant maturity, and now its result is visible in the real-time application of ultrahigh-speed train transportation [5]. For the transportation need, a superconducting maglev system was designed which runs at an ultrahigh speed. The maglev system has successfully been tested at a top speed of around 550 km/hr by the Japanese maglev transportation system, and the commercial service is expected by 2025 [6]. The high-speed maglev Transrapid line in Shanghai and the low-speed Tobu Kyuryo maglev high-speed surface transport

The associate editor coordinating the review of this manuscript and approving it for publication was Zhuang Xu.

line in Nagoya display that the maglev is still in its emerging phases of development [7]. Furthermore, an urban maglev system is being developed to run at speeds up to 110 km/hr between Seoul and Incheon Airport in Korea.

Although maglev technology is heading towards a promising transformation, still maglev system faces some serious challenges while designing the control scheme. First, the maglev dynamics has a non-linear characteristic, open-loop design is unstable, and there is always a threat of unknown and unwanted uncertainties and external disturbances that may destabilize the whole dynamics. So, it is difficult for traditional control algorithms to achieve high-performance criteria, viz. higher precision, better accuracy, fast convergence, and invariance against multiple uncertainties and disruptions.

Recently, several control methodologies have been utilized to regulate and track the position of maglev system, namely model predictive control [2], feedback linearization control [8], robust control [9], intelligent control [10], sliding mode control (SMC) [3], adaptive control [11], etc. These modern schemes enhance the control system response while fulfilling various controller design standards. The key features of an ideal control system are fast response, ease of control design structure, and it should be invariant to disturbance and system uncertainties. The SMC method is an effective robust method for controller design of maglev system since it is widely explored for nonlinear systems with matched uncertainty, provides excellent robust behavior, and has a faster system dynamics response [12], [13], [14], [15], [16].

The SMC control scheme operates in two phases: the reaching mode phase and the sliding mode phase [13]. During the reaching mode, the system solution moves from the initial state to the sliding surface. While the system is in the reaching phase, it is susceptible to system uncertainties, which may result in under-performance of control response [17]. When the system enters the sliding phase, then the output of the system becomes invariant to model uncertainties and disturbances [18]. The concept of integral sliding surface design is proposed to ensure robustness from the initial time $t = 0$. In the integral SMC (ISMC) method, the system enters the sliding phase from $t = 0$ and thus eliminates the reaching phase. The system output slides on the sliding surface from the beginning, or $s = 0$ is achieved from the initial time [19].

Despite having desirable features of the SMC technique, the input chattering phenomenon is its major drawback. Due to the high gain switching function (signum function), the high-frequency component in the discontinuous control law exists. The signum function is employed to suppress the unknown disturbances within the system dynamics and help the solutions to slew over the sliding surface. Although, high-frequency chattering has drastic repercussions if not tackled properly. It could potentially harm the actuator or even destroy it, deteriorate the system performance or eventually destabilize the whole system [20], [21], [22].

Several techniques have been suggested in the literature to overcome chattering, including the boundary layer technique [20], [21] the high-order sliding mode control (HOSMC) technique [23], [24], [25], composite disturbance observer-based technique [26], [27], and integrated extended state observer-based technique [28], [29], to name a few. In the boundary layer method, the effect of chattering is eliminated at the cost of the robust property by employing a continuous estimation of the discontinuous signum function. As a result, the robustness behavior inside the boundary gets compromised. This method is also susceptible to the faster unmodeled dynamics, which might lead to subpar results [30], [31]. On the other hand, the HOSMC strategy solves the chattering issue more efficiently without compromising the robust nature of SMC [32], [33]. However, it is mathematically intensive to design and implement for the real-time application. Further, it requires a differential observer to estimate the higher-order derivatives of state variables [34], [35]. Lastly, the disturbance compensation strategy rejects the disturbance directly without sacrificing SMC performance. In this approach, the gain of switching function is selected to be small to avoid chattering. Consequently, a composite control methodology is developed by integrating the disturbance estimator output with an SMC design [36]. The disturbance compensation technique is primarily based on designing a disturbance observer or estimator. That estimated disturbance is then applied as a feedforward compensation. The extended state observer (ESO), disturbance observer, and the equivalent input disturbance are examples of disturbance estimators [27], [37], [38], [39].

Lately, many integrated SMC techniques for the uncertain maglev system have been reported [40], [41], [42], [43], [44], [45]. A cascaded SMC approach for the maglev system is introduced in [40], and in [41], a terminal sliding mode control (TSMC) method is proposed to enhance convergence rate of the system with finite-time stability. A comprehensive literature review on the recent advancement in the field of sliding mode control strategies has been reported in [46]. A twin-reaching algorithm with the ISMC method is proposed [42] to mitigate chattering from the input at the cost of disturbance attenuation characteristic. In [43], the control for the maglev system employs an adaptive learning method to enhance the system robustness by real-time estimation of unknown disturbances through feed-forward compensation. The implementation of a disturbance and state based SMC control scheme [44] also enhances system robustness. A recent study has integrated an adaptive terminal SMC with an ESO design to obtain an improved reduction in input chattering along with globally uniformly ultimate bounded results [45]. A super-twisting like fractional controller is proposed in [47] for enhancing the performance of surface mounted PMSM system. To reduce the response time for the PMSM drive, a composite control is designed in [48] using the improved non-singular fast terminal sliding mode control. A finite time disturbance observer based backstepping NTSMC control is proposed in [49] with the objective of robustly regulating the speed of PMSM drive. In [50], disturbance observer based adaptive ISMC is discussed to regulate the speed of PMSM system having matched and mismatched disturbance. Only a few results of closed-loop finite-time stability are reported for the maglev system. Although the

finite-time theory ensures a predefined settling time of the state trajectories, its convergence time depends on the initial condition of state variables. Consequently, the convergence time is different for different initial states within the region of attraction [51]. As a result, there is no fixed or generalized predefined convergence time under finite-time stability criteria. The solution to this problem is addressed in [52] by proposing a fixed time convergence theory.

Recently, the fixed-time stability theory has gained significant attention from control researchers due to the generalized fixed-time convergence bound, stronger stability, faster convergence rate, and it is independent of the initial condition within a compact set. One can look into these useful literature review papers for a thorough overview of finite and fixed time stability results [51], [53]. Therefore, fixed/finite time super-twisting high-order sliding mode observers are proposed [54], [55], [56] where the settling time has upper bound values, and it is independent of the initial condition. A fixed-time observer with a dual-limit homogeneous approach is developed in [57]. The application of fixed-time concept to the ESO design has only been studied very recently [58], [59], and there is still a wide area of research for further exploration. Inspired from the above literature, this work investigates the application of a fixed-time ESO merged with a fixed-time integral SMC for the uncertain maglev system.

The major contributions of this paper include:

- The proposed composite control scheme stabilizes the position of levitating ball in the maglev system under model ambiguity and exogenous disturbance.
- The structure of the proposed control algorithm is constituted by integrating the output of fixed-time ESO with the fixed-time integral SMC technique. The ESO design helps estimate and directly cancel the lumped disturbance within a fixed time. As a result, a small gain for discontinuous switching control is enough to ensure the fixed-time stability of the closed-loop states.
- The problem of chattering in the SMC is significantly alleviated from the proposed control input response, thanks to the application of ESO. In addition, the ESO also helps in avoiding the conservative assumption on the upper bound knowledge of total disturbance.
- Moreover, the integral sliding surface for the proposed control design also improves robustness by guaranteeing invariance behavior from the initial time.
- Lastly, detailed theoretical and numerical analysis is presented to prove and validate the stability and effectiveness of the designed methodology.

The organization of remaining paper is as follows. Section II presents the dynamics of the maglev system and the problem statement with few useful Assumptions and Lemmas. Section III demonstrates the proposed composite control design using fixed-time ESO and fixed-time ISMC techniques. The stability analysis using Lyapunov theory for the closed-loop system is established in Section IV. A detailed discussion of the numerical results has been illustrated in Section V and Section VI concludes the paper.

II. DYNAMICS OF MAGLEV SYSTEM

Newton's law of motion can be used to obtain the dynamics of the maglev system, which is expressed as [60]

$$\mathcal{M}\ddot{y} = \mathcal{F} - \mathcal{F}_g, \tag{1}$$

where $\mathcal{M} > 0 \in \mathbb{R}$ represents the levitating ball's mass, $y \in \mathbb{R}$ denotes the displacement in vertical axis, $\mathcal{F} \in \mathbb{R}$ stands for electromagnetic levitation force, and $\mathcal{F}_g \in \mathbb{R}$ is the gravitational force. Equation (1) can also be written as

$$\mathcal{M}\ddot{y} = \mathcal{H}u - \mathcal{M}g, \tag{2}$$

where $\mathcal{H} > 0 \in \mathbb{R}$ is the current amplifier gain that dictates the magnitude of $\mathcal{F}$, $u \in \mathbb{R}$ is the control input, and g is the acceleration due to gravity.

The exact knowledge of system parameters like $\mathcal{M}$ and $\mathcal{H}$ is not always accessible. Therefore, model uncertainties, i.e., $\Delta\mathcal{M}$ and $\Delta\mathcal{H}$, must be considered in (2). Further, the maglev system experiences external disturbances that should also include in the system dynamics. In light of these uncertainties and disturbances, the maglev system equation (2) can be redefined as

$$(\mathcal{M} + \Delta\mathcal{M})\ddot{y} = (\mathcal{H} + \Delta\mathcal{H})u - (\mathcal{M} + \Delta\mathcal{M})g + d_0, \tag{3}$$

where $\Delta\mathcal{M}$ and $\Delta\mathcal{H}$ are the parametric uncertainties of $\mathcal{M}$ and $\mathcal{H}$, respectively, and $d_0 \in \mathbb{R}$ is the surrounding disturbances. All the uncertainties and disturbances can be lumped together as a single variable d, and termed as total disturbance or lumped disturbance. Therefore, Equation (3) can now be written as

$$\ddot{y} = au - g + d, \tag{4}$$

where $a = \mathcal{H}/\mathcal{M} > 0$, and

$$d = \frac{1}{\mathcal{M}}(d_0 + \Delta\mathcal{H}u - \Delta\mathcal{M}g - \Delta\mathcal{M}\ddot{y}). \tag{5}$$

The dynamics equation in double derivative (4) can be simplified into single derivative equations using the state transformation of y by selecting the new variables as

$$x_1 = y, \tag{6a}$$
$$x_2 = \dot{y}. \tag{6b}$$

Now, substituting (6) into the dynamics (4), which yields

$$\dot{x}_1 = x_2, \tag{7a}$$
$$\dot{x}_2 = au - g + d. \tag{7b}$$

Now, for tracking or regulation problem, let us define the relative states as

$$\tilde{x}_1 = x_1 - x_r,$$
$$\tilde{x}_2 = \dot{x}_1 - \dot{x}_r, \tag{8}$$

where x_r is the reference signal. Therefore, the relative error dynamics can be expressed as

$$\dot{\tilde{x}}_1 = \tilde{x}_2, \tag{9a}$$
$$\dot{\tilde{x}}_2 = au - g - \ddot{x}_r + d. \tag{9b}$$

A. PROBLEM STATEMENT

This paper investigates the application of fixed time ESO with the ISMC technique to achieve a fixed time stabilization of the maglev system under total disturbance. To put it another way, the relative state trajectories $\tilde{x}_1$ and $\tilde{x}_2$ must converge to zero within a fixed time t_f under the action of the proposed control algorithm, i.e.,

$$\lim_{t\to t_f} \tilde{x}_1(t) = 0, \tag{10}$$

$$\lim_{t\to t_f} \tilde{x}_2(t) = 0. \tag{11}$$

The following paragraph introduces system assumptions and some useful lemmas that will later be used for stability analysis.

Assumption 1: The measurement of variables x_1 and x_2 are accessible while executing the control law.

Assumption 2: The upper bound of d is finite, i.e., $||\dot{d}|| \leq \bar{d}$, where $\bar{d} \in (0, +\infty)$ is unknown.

Remark 1: The reason for considering the lumped disturbance d in (5) to be bounded is because of the physical design restriction of the maglev system. The position and velocity of levitating ball are finite due to the structural design of maglev system. Further, the electromagnetic control input is derived from a saturated electric power converter, which can only supply a finite output current.

Lemma 1: [52] Consider a continuous system

$$\dot{x}(t) = f(x), \quad x(0) = 0, \quad f(0) = 0. \tag{12}$$

Suppose $\exists$ a Lyapunov function $\mathcal{V}(x) : \mathbb{R}^n \to \mathbb{R}_+ \cup \{0\}$. If the inequality (13) is satisfied with $\eta > 0, \mu > 0, \gamma \in (0, 1)$, and $\zeta > 1$

$$\dot{\mathcal{V}} \leq -\eta \mathcal{V}^{\gamma}(x) - \mu \mathcal{V}^{\zeta}(x). \tag{13}$$

Then, origin is a globally fixed time stable point and the bound of settling time T_b for the state $x(t)$ is given as

$$T_b < T_{\max} := \frac{1}{\eta(1-\gamma)} + \frac{1}{\mu(\zeta-1)}. \tag{14}$$

Lemma 2: [61] Considering a chain of integrator system

$$\begin{aligned} \dot{z}_1 &= z_2, \\ \dot{z}_2 &= z_3, \\ &\cdots \\ \dot{z}_n &= v(t). \end{aligned} \tag{15}$$

Here, the input variable $v(t)$ is given as

$$v(t) = v_{11}(t) + v_{12}(t), \tag{16}$$

where

$$\begin{aligned} v_{11}(t) &= q_1(t) + q_2(t) + \cdots + q_n(t), \\ v_{12}(t) &= w_1(t) + w_2(t) + \cdots + w_n(t), \\ q_i(t) &= -k_i |z_i(t)|^{b_i} \text{sign}(z_i(t)) \text{ for } i = 1, \ldots, n, \\ w_i(t) &= -l_i |z_i(t)|^{c_i} \text{sign}(z_i(t)) \text{ for } i = 1, \ldots, n. \end{aligned} \tag{17}$$

The parameter b_i satisfies $b_i \in (0, 1)$ and holds the relation $b_{i-1} = b_i b_{i+1}/(2b_{i+1} - b_i)$ for $i = 2, \ldots, n$. $b_{n+1} = 1$ and $b_n = b$ where $b \in (1-\epsilon, 1)$ for significantly small value of $\epsilon > 0$. Similarly, $c_i > 1$ for $i = 1, \ldots, n$ satisfies the relation $c_{i-1} = c_i c_{i+1}/(2c_{i+1} - c_i)$, $i = 2, \ldots, n$, $c_{n+1} = 1$ and $c_n = c$ where $c \in (1, 1+\epsilon_1)$ for a small value of $\epsilon_1 > 0$. The controller gains k_i and l_i are selected according to Hurwitz polynomials. Matrices that complies the Hurwitz conditions are given below.

The above system design will achieve a fixed time convergence of state variable $[z_1, z_2, \ldots, z_n]^T$ to zero. The time of convergence T_c satisfies the following inequality

$$T_c \leq \frac{\lambda_{\max}^{\rho}(P_1)}{r_0 \rho} + \frac{1}{r_1 \omega r^{\omega}}, \tag{18}$$

where $\rho = (1-b)/b$, $\omega = (c-1)/c$, $r_0 = \frac{\lambda_{\min}(Q_1)}{\lambda_{\max}(P_1)}$, $r_1 = \frac{\lambda_{\min}(Q_2)}{\lambda_{\max}(P_2)}$, $r \leq \lambda_{\min}(P_2) > 0$, and $\lambda_{\min}(\cdot)$ and $\lambda_{\max}(\cdot)$ represents the minimum and maximum eigenvalues of the corresponding matrices. The parameter Q_1, Q_2, P_1, and P_2 are symmetric positive definite matrices that satisfies the following equations

$$\begin{aligned} P_1 A_1 + A_1^T P_1 &= -Q_1, \\ P_2 A_2 + A_2^T P_2 &= -Q_2, \end{aligned} \tag{19}$$

where

$$A_1 = \begin{bmatrix} 0 & 1 & 0 & \cdots & 0 \\ 0 & 0 & 1 & \cdots & 0 \\ \cdots & & & & \\ 0 & 0 & 0 & \cdots & 1 \\ -k_1 & -k_2 & -k_3 & \cdots & -k_n \end{bmatrix}, \tag{20}$$

$$A_2 = \begin{bmatrix} 0 & 1 & 0 & \cdots & 0 \\ 0 & 0 & 1 & \cdots & 0 \\ \cdots & & & & \\ 0 & 0 & 0 & \cdots & 1 \\ -l_1 & -l_2 & -l_3 & \cdots & -l_n \end{bmatrix}. \tag{21}$$

III. PROPOSED CONTROL DESIGN

This section proposes a composite control scheme by integrating a new fixed-time ESO with a fixed-time integral SMC design. Figure 1 presents the schematic diagram of the proposed control algorithm. The proposed approach has the following benefits. The ESO estimates the total disturbance within a fixed time, and the output of ESO, i.e., the disturbance estimation variable, is fed to the composite control law. Consequently, the ESO output attenuates the majority of system disturbances in fixed time without depending on the large switching gain of discontinuous SMC component. As a result, the input chattering gets alleviated significantly. At the same time, the proposed ISMC achieves a fixed time convergence of sliding surface and relative state. Moreover, it offers the resilience property against unknown disturbances from the very initial time $t = 0$ since there is no reaching phase.

A. FIXED-TIME EXTENDED STATE OBSERVER

This subsection talks about the modeling of fixed-time ESO that estimates the total disturbance in the maglev system within a fixed time. Moreover, the convergence analysis of the given ESO is also illustrated.

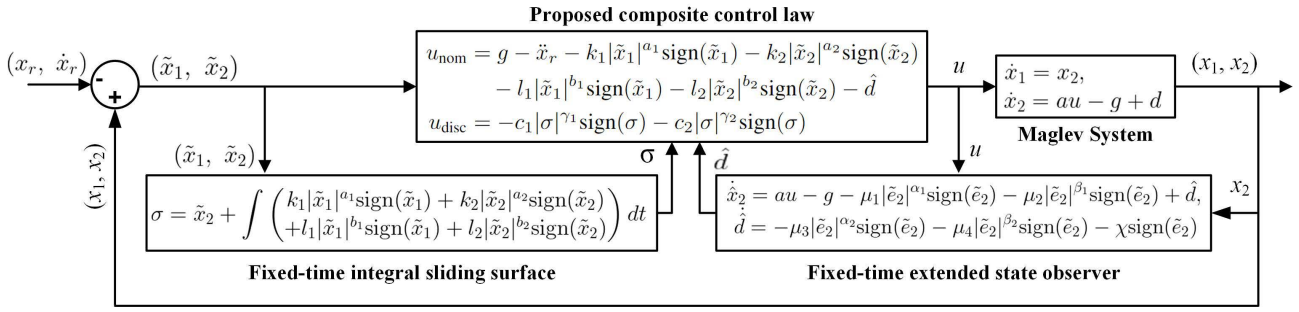

FIGURE 1. Block diagram of the composite ESO-ISMC design.

Suppose $\hat{x}_2$ is the estimate of x_2, which is obtained from the fixed-time ESO. Further, estimation error in x_2 is given as

$$\tilde{e}_2 = \hat{x}_2 - x_2. \tag{22}$$

Then, the equations of fixed-time ESO is defined as [59]

$$\dot{\hat{x}}_2 = au - g - \mu_1|\tilde{e}_2|^{\alpha_1}\text{sign}(\tilde{e}_2) - \mu_2|\tilde{e}_2|^{\beta_1}\text{sign}(\tilde{e}_2) + \hat{d}, \tag{23a}$$

$$\dot{\hat{d}} = -\mu_3|\tilde{e}_2|^{\alpha_2}\text{sign}(\tilde{e}_2) - \mu_4|\tilde{e}_2|^{\beta_2}\text{sign}(\tilde{e}_2) - \chi\text{sign}(\tilde{e}_2), \tag{23b}$$

where $\hat{d}$ is the estimate of disturbance d, $\tilde{e}_2$ denotes the estimation error, the parameter $\alpha_1 \in (0, 1), \beta_1 > 1, \alpha_2 = 2\alpha_1 - 1$, $\beta_2 = 2\beta_1 - 1$, $\chi > \|\dot{d}\|$, and $\mu_1 > 0$, $\mu_2 > 0$, $\mu_3 > 0$, and $\mu_4 > 0$ are the observer gains to be designed.

The following theorem establishes the fixed time convergence of disturbance estimation error to zero.

Theorem 1: Considering the maglev dynamics (7) with Assumption 2. The given fixed-time ESO (23) will estimate the total disturbance d within a fixed time. Further, the estimation error will converge to the origin within the following convergence time bound T_c

$$T_c \leq \frac{\lambda_{\max}(A_1)^{(1-\alpha_1)}}{\lambda_1(1-\alpha_1)} + \frac{1}{\lambda_2(\beta_1 - 1)\bar{w}^{(\beta_1 - 1)}}, \tag{24}$$

where $\lambda_1 = \frac{\lambda_{\min}(Q_1)}{\lambda_{\max}(A_1)}$, $\lambda_2 = \frac{\lambda_{\min}(Q_2)}{\lambda_{\max}(A_2)}$, $\lambda_{\min} \geq \bar{w} > 0$, and Q_1, Q_2, A_1, and A_2 are positive definite matrices that satisfies

$$\begin{aligned} A_1P_1 + P_1^TA_1 &= -Q_1, \\ A_2P_2 + P_2^TA_2 &= -Q_2, \end{aligned} \tag{25}$$

where

$$P_1 = \begin{bmatrix} -\mu_1 & 1 \\ -\mu_3 & 0 \end{bmatrix}, \quad P_2 = \begin{bmatrix} -\mu_2 & 1 \\ -\mu_4 & 0 \end{bmatrix}. \tag{26}$$

Proof: Defining the error variables as

$$\tilde{e}_2 = \hat{x}_2 - x_2, \tag{27a}$$

$$\tilde{d} = \hat{d} - d. \tag{27b}$$

Error dynamics of x_2 can be defined using (23) and (27) as

$$\begin{aligned} \dot{\tilde{e}}_2 &= \dot{\hat{x}}_2 - \dot{x}_2, \\ &= au - g - \mu_1|\tilde{e}_2|^{\alpha_1}\text{sign}(\tilde{e}_2) - \mu_2|\tilde{e}_2|^{\beta_1}\text{sign}(\tilde{e}_2) \\ &\quad + \hat{d} - au + g - d, \\ &= (\hat{d} - d) - \mu_1|\tilde{e}_2|^{\alpha_1}\text{sign}(\tilde{e}_2) - \mu_2|\tilde{e}_2|^{\beta_1}\text{sign}(\tilde{e}_2), \\ &= \tilde{d} - \mu_1|\tilde{e}_2|^{\alpha_1}\text{sign}(\tilde{e}_2) - \mu_2|\tilde{e}_2|^{\beta_1}\text{sign}(\tilde{e}_2). \end{aligned} \tag{28}$$

Similarly, the disturbance estimation error dynamics is

$$\begin{aligned} \dot{\tilde{d}} &= \dot{\hat{d}} - \dot{d}, \\ &= -\mu_3|\tilde{e}_2|^{\alpha_2}\text{sign}(\tilde{e}_2) - \mu_4|\tilde{e}_2|^{\beta_2}\text{sign}(\tilde{e}_2) - \dot{d}. \end{aligned} \tag{29}$$

Therefore, the relative dynamics of ESO is given as

$$\begin{aligned} \dot{\tilde{e}}_2 &= \tilde{d} - \mu_1|\tilde{e}_2|^{\alpha_1}\text{sign}(\tilde{e}_2) - \mu_2|\tilde{e}_2|^{\beta_1}\text{sign}(\tilde{e}_2), \\ \dot{\tilde{d}} &= -\mu_3|\tilde{e}_2|^{\alpha_2}\text{sign}(\tilde{e}_2) - \mu_4|\tilde{e}_2|^{\beta_2}\text{sign}(\tilde{e}_2) - \dot{d}. \end{aligned} \tag{30}$$

Now, according to the fixed-time convergence analysis of non-recursive observer given in [54], the error dynamics $\tilde{e}_2$ and $\tilde{d}$ is guaranteed to converge to zero in a fixed time. As a result, the lumped disturbance can be estimated within a fixed time bound T_c, which is defined in (24). Thus, the proof of Theorem 1 is completed. □

In the next part, the output of fixed-time ESO, i.e., the variable $\hat{d}$, is combined with the fixed-time ISMC structure to formulate the proposed composite control law for the maglev system.

B. COMPOSITE CONTROL STRUCTURE USING FIXED-TIME ESO AND ISMC

First, an integral sliding surface is constructed using the system error variables. Then, the fixed-time integral sliding mode control is designed using the inverse dynamics technique by taking the derivative of the sliding surface. Later, the output of fixed-time ESO is combined with the given integral sliding mode control law to obtain the proposed composite control scheme.

Inspired from [62], the structure of the integral sliding surface $\sigma \in \mathbb{R}$ is given as

$$\sigma = \tilde{x}_2 + \int \left(k_1|\tilde{x}_1|^{a_1}\text{sign}(\tilde{x}_1) + k_2|\tilde{x}_2|^{a_2}\text{sign}(\tilde{x}_2) + l_1|\tilde{x}_1|^{b_1}\text{sign}(\tilde{x}_1) + l_2|\tilde{x}_2|^{b_2}\text{sign}(\tilde{x}_2)\right) dt \tag{31}$$

where $a_1 \in (0, 1)$, $a_2 \in (0, 1)$, $b_1 > 1$, and $b_2 > 1$ are exponents, and they are designed as per the condition of Lemma 2. Further, gain parameters $k_1 > 0$, $k_2 > 0$, $l_1 > 0$, and $l_2 > 0$ need to be designed.

The time derivative of σ yields

$$\begin{aligned} \dot{\sigma} &= \dot{\tilde{x}}_2 + k_1|\tilde{x}_1|^{a_1}\text{sign}(\tilde{x}_1) + k_2|\tilde{x}_2|^{a_2}\text{sign}(\tilde{x}_2) \\ &\quad + l_1|\tilde{x}_1|^{b_1}\text{sign}(\tilde{x}_1) + l_2|\tilde{x}_2|^{b_2}\text{sign}(\tilde{x}_2). \end{aligned} \tag{32}$$

Substituting $\dot{\tilde{x}}_2$ from (9b) into (32) gives

$$\dot{\sigma} = au - g - \ddot{x}_r + k_1|\tilde{x}_1|^{a_1}\text{sign}(\tilde{x}_1) + k_2|\tilde{x}_2|^{a_2}\text{sign}(\tilde{x}_2) + l_1|\tilde{x}_1|^{b_1}\text{sign}(\tilde{x}_1) + l_2|\tilde{x}_2|^{b_2}\text{sign}(\tilde{x}_2) + d. \quad (33)$$

The proposed composite control law u comprises two parts: nominal component u_{nom} and discontinuous component u_{disc}. The objective of nominal control is to cancel all the unwanted parts of the closed-loop dynamics and drive the system trajectories to the intended position and velocity. Meanwhile, the discontinuous control achieves the fixed time convergence result and attenuates the impact of remaining uncertainties and disturbances from the ESO approach.

The proposed fixed-time ESO-ISMC law u is designed using generalized dynamic inversion method as

$$u = \frac{1}{a}(u_{\text{nom}} + u_{\text{disc}}), \quad (34)$$

where

$$u_{\text{nom}} = g - \ddot{x}_r - k_1|\tilde{x}_1|^{a_1}\text{sign}(\tilde{x}_1) - k_2|\tilde{x}_2|^{a_2}\text{sign}(\tilde{x}_2) - l_1|\tilde{x}_1|^{b_1}\text{sign}(\tilde{x}_1) - l_2|\tilde{x}_2|^{b_2}\text{sign}(\tilde{x}_2) - \hat{d}, \quad (35)$$

$$u_{\text{disc}} = -c_1|\sigma|^{\gamma_1}\text{sign}(\sigma) - c_2|\sigma|^{\gamma_2}\text{sign}(\sigma), \quad (36)$$

where $c_1 > 0$ and $c_2 > 0$ are small gains, which handle the residual errors and determine the rate of convergence. Further, parameters γ_1 and γ_2 are the exponents that satisfy $0 < \gamma_1 < 1$ and $\gamma_2 > 1$.

Remark 2: Since the proposed scheme is a combination of fixed-time ESO and fixed-time ISMC, it enjoys the benefits of both approaches. Therefore, the ESO helps in estimating the system disturbance within a fixed time and the observed disturbance attenuates the actual disturbance using the feed-forward compensation. Thus, it avoids the application of a large value of switching gain in the ISMC approach, which in turn reduces the input chattering. In addition, the proposed sliding surface structure ensures the fixed time convergence of relative state trajectories. Moreover, the integral surface design enables the closed-loop system to start from the sliding phase from the initial time. As a result, the robustness of the proposed methodology is reinforced from the starting time, which is also beneficial since ESO initially takes a short time to estimate the disturbance.

Remark 3: The parameters c_1 and c_2 are positive constants that dictate the convergence time of system trajectories. However, large values of c_1 and c_2 can create input chattering. Therefore, one needs to make a trade-off between the desired rate of convergence and the allowable limit of chattering.

IV. CLOSED-LOOP STABILITY ANALYSIS

Theorem 2: Consider the sliding dynamics (33) under Assumption 2 and the composite control law (34). The proposed methodology will attain the sliding phase ($sigma = 0$) within a fixed time. Likewise, the error states will also force to the origin in a fixed time.

Proof: The proof of the above theorem is given in two parts. In the first part, sliding surface convergence is established, and the second part proves the fixed time convergence of the relative states.

Part I: Defining a Lyapunov function V_1 as

$$V_1 = \frac{1}{2}\sigma^2. \quad (37)$$

The derivative of V_1 with respect to time is

$$\dot{V}_1 = \sigma\dot{\sigma}. \quad (38)$$

Putting $\dot{\sigma}$ from (33) to (38) yields

$$\dot{V}_1 = \sigma\left(au - g + k_1|\tilde{x}_1|^{a_1}\text{sign}(\tilde{x}_1) + k_2|\tilde{x}_2|^{a_2}\text{sign}(\tilde{x}_2) + l_1|\tilde{x}_1|^{b_1}\text{sign}(\tilde{x}_1) + l_2|\tilde{x}_2|^{b_2}\text{sign}(\tilde{x}_2) - \ddot{x}_r + d\right). \quad (39)$$

Substituting the expression of u from (35) and (36) into (39)

$$\dot{V}_1 = \sigma(\underbrace{d - \hat{d}}_{\tilde{d}} - c_1|\sigma|^{\gamma_1}\text{sign}(\sigma) - c_2|\sigma|^{\gamma_2}\text{sign}(\sigma)). \quad (40)$$

It has already been established in Theorem 1 that when time $t > T_c$ the disturbance estimation error goes to zero, i.e., $\tilde{d} = 0$. Therefore, Equation (40) can be written as

$$\begin{aligned}\dot{V}_1 &= \sigma(-c_1|\sigma|^{\gamma_1}\text{sign}(\sigma) - c_2|\sigma|^{\gamma_2}\text{sign}(\sigma)),\\ &= -c_1|\sigma|^{\gamma_1+1} - c_2|\sigma|^{\gamma_2+1},\\ &= -c_1 2^{\frac{\gamma_1+1}{2}}\left(\frac{\sigma^2}{2}\right)^{\frac{\gamma_1+1}{2}} - c_2 2^{\frac{\gamma_2+1}{2}}\left(\frac{\sigma^2}{2}\right)^{\frac{\gamma_2+1}{2}},\\ \dot{V}_1 &\le -\eta_1 V_1^{\xi_1} - \eta_2 V_1^{\xi_2}, \end{aligned} \quad (41)$$

where $\eta_i = 2^{\frac{\gamma_i+1}{2}}c_i > 0$, for $i = 1, 2$, $\xi_1 = \frac{\gamma_1+1}{2} \in (0, 1)$, and $\xi_2 = \frac{\gamma_2+1}{2} > 1$.

In view of inequality given in Lemma 1, the above equation (41) holds the same condition as (13). Therefore, it can be claimed that the sliding surface will converge to zero within a fixed time. In other words, the sliding phase will achieve in a fixed time.

Part II: Since both σ and $\dot{\sigma}$ become zero when the sliding phase is achieved. Therefore, $\dot{\sigma}$ from (32) can be written as

$$\dot{\sigma} = \dot{\tilde{x}}_2 + k_1|\tilde{x}_1|^{a_1}\text{sign}(\tilde{x}_1) + k_2|\tilde{x}_2|^{a_2}\text{sign}(\tilde{x}_2) + l_1|\tilde{x}_1|^{b_1}\text{sign}(\tilde{x}_1) + l_2|\tilde{x}_2|^{b_2}\text{sign}(\tilde{x}_2) = 0. \quad (42)$$

Equation (42) can also be written as

$$\dot{\tilde{x}}_2 = -k_1|\tilde{x}_1|^{a_1}\text{sign}(\tilde{x}_1) - k_2|\tilde{x}_2|^{a_2}\text{sign}(\tilde{x}_2) - l_1|\tilde{x}_1|^{b_1}\text{sign}(\tilde{x}_1) - l_2|\tilde{x}_2|^{b_2}\text{sign}(\tilde{x}_2). \quad (43)$$

The reduced order system after achieving the sliding phase can be written as

$$\begin{aligned}\dot{\tilde{x}}_1 &= \tilde{x}_2,\\ \dot{\tilde{x}}_2 &= \underbrace{-k_1|\tilde{x}_1|^{a_1}\text{sign}(\tilde{x}_1) - k_2|\tilde{x}_2|^{a_2}\text{sign}(\tilde{x}_2)}_{v_1}\\ &\quad \underbrace{-l_1|\tilde{x}_1|^{b_1}\text{sign}(\tilde{x}_1) - l_2|\tilde{x}_2|^{b_2}\text{sign}(\tilde{x}_2)}_{v_2}. \end{aligned} \quad (44)$$

Therefore, Equation (44) can be expressed as

$$\begin{aligned}\dot{\tilde{x}}_1 &= \tilde{x}_2,\\ \dot{\tilde{x}}_2 &= v_1 + v_2, \end{aligned} \quad (45)$$

where

$$v_1 = -k_1|\tilde{x}_1|^{a_1}\text{sign}(\tilde{x}_1) - k_2|\tilde{x}_2|^{a_2}\text{sign}(\tilde{x}_2). \quad (46)$$

$$v_2 = -l_1|\tilde{x}_1|^{b_1}\text{sign}(\tilde{x}_1) - l_2|\tilde{x}_2|^{b_2}\text{sign}(\tilde{x}_2). \quad (47)$$

Equation (45) holds the condition of Lemma 2. Thus, the relative states $\tilde{x}_1$ and $\tilde{x}_2$ will go to zero in a fixed time, as assured in Lemma 2. Hence, the proof of Theorem 2 is completed. □

Remark 4: While implementing the proposed controller, the following points need to be considered:

i) The initial condition of integral sliding surface in (31) should be selected such that $\sigma(0) = 0$. Therefore, the initial value of integral is selected as $-\tilde{x}_2(0)$.
ii) The switching gain of discontinuous control, i.e., c_1 and c_2, should be skillfully selected to avoid the chattering phenomenon and also achieve the desired convergence rate.
iii) Similarly, the gains of fixed-time ESO also need to be appropriately chosen in order to quickly estimate and compensate the disturbance.

V. NUMERICAL ANALYSIS

In order to verify the effectiveness of the proposed composite control methodology, the numerical simulation is carried out for the maglev system in MATLAB®. The maglev system is comprised of electrical and mechanical units, including an electromagnet, levitating ball, laser sensor, and a power converter. The position of the levitating ball is regulated by controlling the electric current through the power converter. Meanwhile, the laser sensor feeds the relative position measurement of the ball from the coil to the control processing unit. The open-loop maglev system is unstable and highly susceptible to external perturbations and uncertainties. Therefore, the task of the proposed investigation is to regulate the position of a levitating ball in the maglev system under the influence of uncertainties and disturbances. The performance of the proposed scheme, i.e., fixed time ESO based fixed time ISMC (ESO-ISMC), is also compared with an ISMC technique [63] and nonsingular fast terminal SMC (NTSMC) approach [64].

In this paper, the parameters of the maglev system are taken as: mass of levitating ball $\mathcal{M} = 450$g, the current amplifier gain $\mathcal{H} = 1000$, and the acceleration due to gravity $g = 9.81\ m/sec^2$. Besides, for the purpose of simulation, the model uncertainty is considered as $\Delta\mathcal{M} = 0.1\mathcal{M}$ and $\Delta\mathcal{H} = 0.1\mathcal{H}$. The surrounding time varying disturbance is considered as

$$d_0 = 0.3\cos(0.2t) + 0.2\sin(0.5t).$$

The initial and reference values of the state trajectories are chosen as

$$x_1(0) = 0\text{ cm} \quad \text{and} \quad x_2(0) = 0.5,$$
$$x_r = 1.5\text{ cm} \quad \text{and} \quad \dot{x}_r = 0.$$

Parameter values of the composite control design are given in Table 1.

TABLE 1. Composite control design parameters.

Parameter	Value	Parameter	Value	Parameter	Value
μ_1	10	α_1	0.9	k_1	4
μ_2	50	α_2	0.8	k_2	4
μ_3	50	β_1	1.1	l_1	4
μ_4	100	β_2	1.2	l_2	4
a_1	0.8	a_2	1.1	b_1	0.8
b_2	1.1	χ	0.6	γ_1	0.8
γ_2	1.2	c_1	1.8	c_2	2

The responses of state variables and the error state trajectories are respectively illustrated in Fig. 2 and Fig. 3. It is evident from Fig. 2 that the position of levitating ball (x_1) reaches the desired set value, i.e., 1.5 cm under all the schemes. However, the proposed fixed-time ESO-ISMC algorithm achieves faster convergence than the other two approaches. The convergence time of state trajectory is evaluated when the relative state settles down to the bound of $\|\tilde{x}\| \leq 1 \times 10^{-2}$ and stays within this set. Therefore, the proposed controller (34) takes 2.72 s for convergence, whereas scheme of [63] and [64] accomplish the same bound in 7.87 s and 3.57 s, respectively. Similarly, the velocity of the levitating ball (x_2) converges to the origin faster under the composite fixed time ESO-ISMC scheme than in the other two methods (see in bottom plot of Fig. 2). The settling time of relative velocity under these schemes are also given in Table 2.

Moreover, the regulation performance is further illustrated using relative state responses of $\tilde{x}_1$ and $\tilde{x}_2$ in Fig. 3. The errors are approaching zero faster under the proposed composite control than in the ISMC and NTSMC schemes, as seen in this figure. The zoomed-in plots of steady-state response are also shown in Fig. 3, which depicts that the proposed algorithm has a better error convergence bound. The residual bound of error trajectories under different schemes is tabulated in Table 2. The composite fixed time ESO-ISMC scheme effectively converges the $\|\tilde{x}\|$ to a narrower bound, i.e., 3.3×10^{-5}, which is least among the other two approaches. One more thing to notice that the chattering effect is also not present in the relative velocity response under the proposed scheme (visible in zoomed plot of Fig. 3) thanks to the application of fixed-time ESO. On the other hand, under NTSMC [64] and ISMC [63] responses, the effect of chattering is visible in the steady-state response of $\tilde{x}_2$. The elaborated discussion on input chattering and its analysis under these schemes are presented in the later paragraph.

Figure 4 shows the sliding surface response under the proposed composite control technique, the NTSMC scheme [64], and the ISMC [63] design. Note that due to the application of an integral sliding surface, the reaching phase is almost negligible in the composite and the ISMC [63] schemes and the surface starts from zero. Although the convergence of sliding trajectories under NTSMC scheme seems to be fast, the proposed composite scheme has a better transient and steady-state behavior with no fluctuations in its response, as seen in the zoomed-in plot in Fig. 4. On the other hand, the ISMC and NTSMC schemes experience a chattering effect throughout the sliding phase response due to the

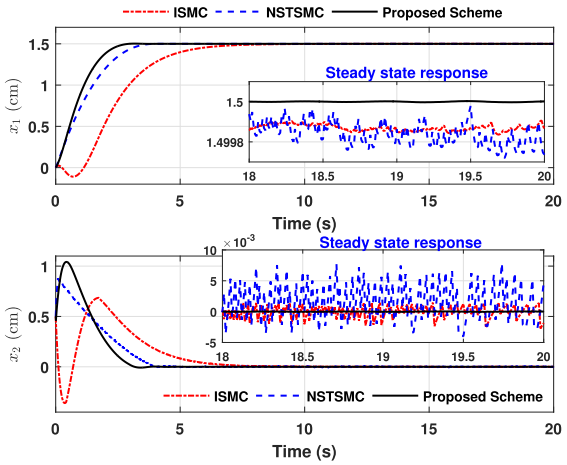

FIGURE 2. State trajectory response under different control schemes.

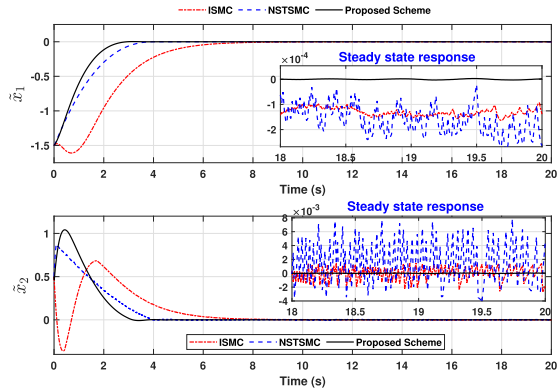

FIGURE 3. Relative state response under different control schemes.

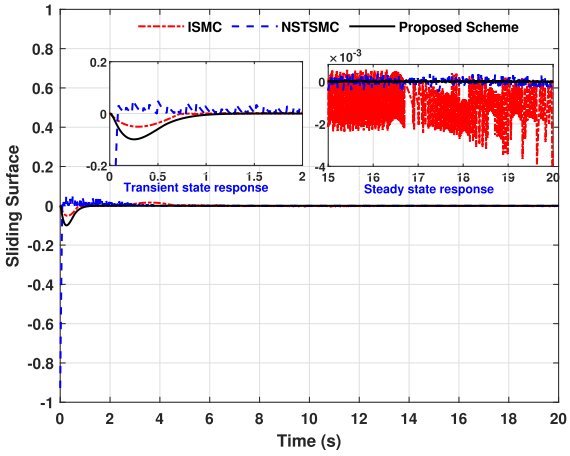

FIGURE 4. Sliding surface response under different control schemes.

application of high gain switching in the discontinuous control component.

The time history of control input response for these three schemes is shown in Fig. 5. Simply by looking at these responses, it is evident that the proposed scheme has significantly eliminated the input chattering from its control response, thanks to the use of ESO. On the contrary, the NTSMC has the highest magnitude of chattering. The reason

TABLE 2. Performance measures under different control schemes.

Measures	Proposed	ISMC [63]	NTSMC [64]
$T_{settling}$ of $\tilde{x}_1$ (s)	2.72	7.87	3.57
$T_{settling}$ of $\tilde{x}_2$ (s)	3.07	8.07	3.89
Settling bound $\|\tilde{\boldsymbol{x}}\|$	3.3×10^{-5}	1.9×10^{-3}	4.7×10^{-3}
EI (A^2)	390.106	392.486	415.618
TV (A)	9.9792	1.41×10^2	1.31×10^3

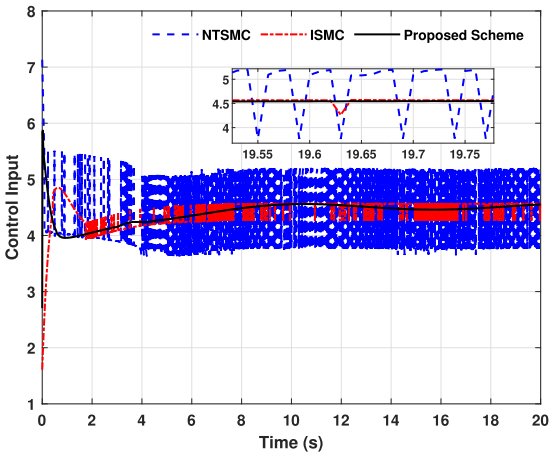

FIGURE 5. Control input response under different control schemes.

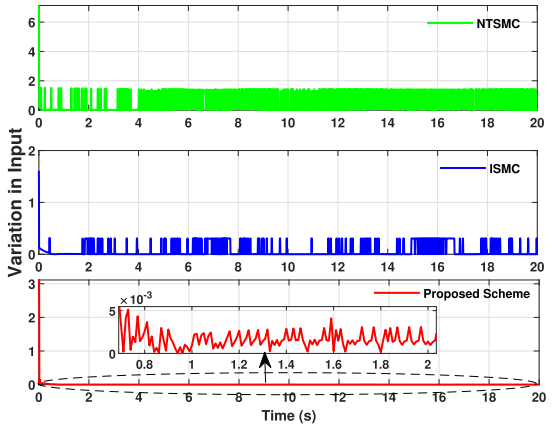

FIGURE 6. Time history of total input variation for three control schemes.

for the presence of chattering in [63] and [64] is the direct dependence on the large gain switching control to attenuate the effect of total disturbance. Moreover, two performance measure functions are evaluated for these control schemes to validate the effective performance of the proposed algorithm quantitatively. Therefore, first, the energy consumed by these control laws is calculated using the energy index (EI) function, defined as

$$\mathrm{EI} = \int_0^{20} |u(t)|^2 \, dt. \tag{48}$$

The calculated EI values are given in Table 2, which illustrates that the proposed method (34) utilizes the least amount of control effort than the algorithms of [63] and [64].

Secondly, the quantitative analysis for the reduction in input chattering is measured using the total variation (TV)

of input function, which is expressed as

$$\mathrm{TV} = \sum_{i=0}^{n} |u(i+1) - u(i)|\,, \tag{49}$$

where n represents the total number of control input samples for the complete simulation time. The TV values of these control strategies are also tabulated in Table 2, which shows that the proposed ESO-ISMC scheme has the least TV value. This implies that the proposed composite law has minimal input variation or, in other words, the chattering effect has been significantly suppressed. In contrast, the other two approaches have considerable chattering; therefore, the TV values are high in these two comparative methods. The above observation can also be visualize through the time history response of TV, which is shown in Fig. 6. It is obvious from the TV plot that the proposed control has a minimum amplitude of variation throughout the simulation than the NTSMC and the ISMC methods.

VI. CONCLUSION

This paper develops a composite robust control law using fixed-time ESO and ISMC for regulating the position of levitating ball in a maglev system under model uncertainties and disturbances. The fixed-time ESO provides three benefits, i.e., (i) estimates total disturbance within a fixed time without knowing the upper limit of disturbance, (ii) compensates total disturbance as feed-forward compensation, and (iii) significantly reduces chattering from ISMC design. Meanwhile, the proposed ISMC ensures fixed-time convergence of closed-loop signals, better transient response, and equips with better invariance property because of no reaching phase. The Lyapunov theory establishes the theoretical results, which affirms the fixed time convergence of both sliding and error states. Lastly, a comparative simulation analysis illustrates the efficacy of the proposed algorithm with respect to the state-of-the-art methods. In the future extension, the proposed methodology will be realized in the hardware setup to further support its real-time implementation.

REFERENCES

[1] D. M. Rote, "Magnetic levitation," in *Encyclopedia of Energy*, C. J. Cleveland, Ed. New York, NY, USA: Elsevier, 2004, pp. 691–703.
[2] T. Bächle, S. Hentzelt, and K. Graichen, "Nonlinear model predictive control of a magnetic levitation system," *Control Eng. Pract.*, vol. 21, no. 9, pp. 1250–1258, Sep. 2013.
[3] H.-W. Lee, K.-C. Kim, and J. Lee, "Review of Maglev train technologies," *IEEE Trans. Magn.*, vol. 42, no. 7, pp. 1917–1925, Jul. 2006.
[4] S. Xu and J. Fang, "A novel conical active magnetic bearing with claw structure," *IEEE Trans. Magn.*, vol. 50, no. 5, pp. 1–8, May 2014.
[5] L. Yan, "Development and application of the Maglev transportation system," *IEEE Trans. Appl. Supercond.*, vol. 18, no. 2, pp. 92–99, Jun. 2008.
[6] K. Sawada, "Outlook of the superconducting Maglev," *Proc. IEEE*, vol. 97, no. 11, pp. 1881–1885, Nov. 2009.
[7] Y. Luguang, "Progress of the Maglev transportation in China," *IEEE Trans. Appl. Supercond.*, vol. 16, no. 2, pp. 1138–1141, Jun. 2006.
[8] Y. Qin, H. Peng, W. Ruan, J. Wu, and J. Gao, "A modeling and control approach to magnetic levitation system based on state-dependent ARX model," *J. Process Control*, vol. 24, no. 1, pp. 93–112, Jan. 2014.
[9] T. Glück, W. Kemmetmüller, C. Tump, and A. Kugi, "A novel robust position estimator for self-sensing magnetic levitation systems based on least squares identification," *Control Eng. Pract.*, vol. 19, no. 2, pp. 146–157, 2011.
[10] J. de Jesús Rubio, L. Zhang, E. Lughofer, P. Cruz, A. Alsaedi, and T. Hayat, "Modeling and control with neural networks for a magnetic levitation system," *Neurocomputing*, vol. 227, pp. 113–121, Mar. 2017.
[11] Z.-J. Yang and M. Tateishi, "Adaptive robust nonlinear control of a magnetic levitation system," *Automatica*, vol. 37, no. 7, pp. 1125–1131, Jul. 2001.
[12] V. Utkin, "Variable structure systems with sliding modes," *IEEE Trans. Autom. Control*, vol. AC-22, no. 2, pp. 212–222, Apr. 1977.
[13] Y. Shtessel, C. Edwards, L. Fridman, and A. Levant, *Sliding Mode Control and Observation*, vol. 10. New York, NY, USA: Springer, 2014.
[14] J. Liu and X. Wang, *Advanced Sliding Mode Control for Mechanical Systems*. Berlin, Germany: Springer, 2012.
[15] C. S. Chin and C. Wheeler, "Sliding-mode control of an electromagnetic actuated conveyance system using contactless sensing," *IEEE Trans. Ind. Electron.*, vol. 60, no. 11, pp. 5315–5324, Nov. 2012.
[16] S. M. Amrr, A. Banerjee, and M. Nabi, "Time-energy efficient path tracking for spacecraft in finite-time under input saturation," in *Proc. 28th Medit. Conf. Control Autom. (MED)*, Sep. 2020, pp. 230–235.
[17] Y.-S. Lu and J.-S. Chen, "Design of a global sliding-mode controller for a motor drive with bounded control," *Int. J. Control*, vol. 62, no. 5, pp. 1001–1019, Nov. 1995.
[18] J. Y. Hung, W. Gao, and J. C. Hung, "Variable structure control: A survey," *IEEE Trans. Ind. Electron.*, vol. 40, no. 1, pp. 2–22, Feb. 1993.
[19] S. M. Amrr, M. Nabi, and P. M. Tiwari, "A fault-tolerant attitude tracking control of spacecraft using an anti-unwinding robust nonlinear disturbance observer," *Proc. Inst. Mech. Eng. G, J. Aerosp. Eng.*, vol. 233, no. 16, pp. 6005–6018, Dec. 2019.
[20] J. Guldner and V. Utkin, "The chattering problem in sliding mode systems," in *Proc. 14th Int. Symp. Math. Theory Netw. Syst. (MTNS)*, Jun. 2000, pp. 1–8.
[21] A. Levant, "Chattering analysis," *IEEE Trans. Autom. Control*, vol. 55, no. 6, pp. 1380–1389, Jun. 2010.
[22] Y. Pan, Y. H. Joo, and H. Yu, "Discussions on smooth modifications of integral sliding mode control," *Int. J. Control, Autom. Syst.*, vol. 16, no. 2, pp. 586–593, Apr. 2018.
[23] S. Laghrouche, F. Plestan, and A. Glumineau, "Higher order sliding mode control based on integral sliding mode," *Automatica*, vol. 43, no. 3, pp. 531–537, Mar. 2007.
[24] S. Saha, S. M. Amrr, A. S. Saidi, A. Banerjee, and M. Nabi, "Finite-time adaptive higher-order SMC for the nonlinear five DOF active magnetic bearing system," *Electronics*, vol. 10, no. 11, p. 1333, Jun. 2021.
[25] S. M. Amrr, R. Sarkar, A. Banerjee, A. S. Saidi, and M. U. Nabi, "Fault-tolerant finite-time adaptive higher order sliding mode control with optimized parameters for attitude stabilization of spacecraft," *Int. J. Robust Nonlinear Control*, vol. 32, no. 5, pp. 2845–2863, Mar. 2022.
[26] Y. Li, Q. Zheng, and L. Yang, "Design of robust sliding mode control with disturbance observer for multi-axis coordinated traveling system," *Comput. Math. Appl.*, vol. 64, no. 5, pp. 759–765, Sep. 2012.
[27] S. M. Amrr and M. Nabi, "Finite-time fault tolerant attitude tracking control of spacecraft using robust nonlinear disturbance observer with anti-unwinding approach," *Adv. Space Res.*, vol. 66, no. 7, pp. 1659–1671, Oct. 2020.
[28] R. Cui, L. Chen, C. Yang, and M. Chen, "Extended state observer-based integral sliding mode control for an underwater robot with unknown disturbances and uncertain nonlinearities," *IEEE Trans. Ind. Electron.*, vol. 64, no. 8, pp. 6785–6795, Aug. 2017.
[29] A. Sharma, S. M. Amrr, M. Nabi, and S. Banerjee, "Extended state observer based integral sliding mode control of maglev systems with enhanced chattering alleviation," in *Proc. 7th Indian Control Conf. (ICC)*, Dec. 2021, pp. 242–247.
[30] J.-J. E. Slotine and W. Li, *Applied Nonlinear Control*, 1st ed. Englewood Cliffs, NJ, USA: Prentice-Hall, 1991.
[31] I. M. Boiko, "Chattering in sliding mode control systems with boundary layer approximation of discontinuous control," *Int. J. Syst. Sci.*, vol. 44, no. 6, pp. 1126–1133, Jun. 2013.
[32] V. Utkin, "Discussion aspects of high-order sliding mode control," *IEEE Trans. Autom. Control*, vol. 61, no. 3, pp. 829–833, Mar. 2016.
[33] V. Utkin, A. Poznyak, Y. Orlov, and A. Polyakov, "Conventional and high order sliding mode control," *J. Franklin Inst.*, vol. 357, no. 15, pp. 10244–10261, 2020.
[34] L. Fridman, J. A. Moreno, B. Bandyopadhyay, S. Kamal, and A. Chalanga, "Continuous nested algorithms: The fifth generation of sliding mode controllers," in *Recent Advances in Sliding Modes: From Control to Intelligent Mechatronics*. Cham, Switzerland: Springer, 2015, pp. 5–35.

[35] J. Davila, L. M. Fridman, and A. Levant, "Second-order sliding-mode observer for mechanical systems," *IEEE Trans. Autom. Control*, vol. 50, no. 11, pp. 1785–1789, Nov. 2005.
[36] S. M. Amrr, A. Banerjee, and M. Nabi, "Time-energy efficient finite time attitude tracking control of spacecraft using disturbance observer," *IFAC-PapersOnLine*, vol. 53, no. 2, pp. 5964–5969, 2020.
[37] J. Han, "From PID to active disturbance rejection control," *IEEE Trans. Ind. Electron.*, vol. 56, no. 3, pp. 900–906, Mar. 2009.
[38] L. Yu, J. Huang, and S. Fei, "Robust switching control of the direct-drive servo control systems based on disturbance observer for switching gain reduction," *IEEE Trans. Circuits Syst. II, Exp. Briefs*, vol. 66, no. 8, pp. 1366–1370, Nov. 2019.
[39] J.-H. She, X. Xin, and Y. Pan, "Equivalent-input-disturbance approach—Analysis and application to disturbance rejection in dual-stage feed drive control system," *IEEE/ASME Trans. Mechatronics*, vol. 16, no. 2, pp. 330–340, Apr. 2011.
[40] Y. Eroğlu and G. Ablay, "Cascade sliding mode–based robust tracking control of a magnetic levitation system," *Proc. Inst. Mech. Eng. I, J. Syst. Control Eng.*, vol. 230, no. 8, pp. 851–860, Sep. 2016.
[41] N. Boonsatit and C. Pukdeboon, "Adaptive fast terminal sliding mode control of magnetic levitation system," *J. Control, Autom. Electr. Syst.*, vol. 27, no. 4, pp. 359–367, Aug. 2016.
[42] J. Pan, W. Li, and H. P. Zhang, "Control algorithms of magnetic suspension systems based on the improved double exponential reaching law of sliding mode control," *Int. J. Control, Automat. Syst.*, vol. 16, no. 6, pp. 2878–2887, Dec. 2018.
[43] F. J. Lin, S. Y. Chen, and K. K. Shyu, "Robust dynamic sliding-mode control using adaptive RENN for magnetic levitation system," *IEEE Trans. Neural Netw.*, vol. 20, no. 6, pp. 938–951, Jun. 2009.
[44] D. Ginoya, C. M. Gutte, P. Shendge, and S. Phadke, "State-and-disturbance-observer-based sliding mode control of magnetic levitation systems," *Trans. Inst. Meas. Control*, vol. 38, no. 6, pp. 751–763, Jun. 2016.
[45] J. Wang, L. Zhao, and L. Yu, "Adaptive terminal sliding mode control for magnetic levitation systems with enhanced disturbance compensation," *IEEE Trans. Ind. Electron.*, vol. 68, no. 1, pp. 756–766, Jan. 2021.
[46] J. Hu, H. Zhang, H. Liu, and X. Yu, "A survey on sliding mode control for networked control systems," *Int. J. Syst. Sci.*, vol. 52, no. 6, pp. 1129–1147, Apr. 2021.
[47] Q. Hou, S. Ding, X. Yu, and K. Mei, "A super-twisting-like fractional controller for SPMSM drive system," *IEEE Trans. Ind. Electron.*, vol. 69, no. 9, pp. 9376–9384, Sep. 2022.
[48] B. Xu, L. Zhang, and W. Ji, "Improved non-singular fast terminal sliding mode control with disturbance observer for PMSM drives," *IEEE Trans. Transport. Electrific.*, vol. 7, no. 4, pp. 2753–2762, Dec. 2021.
[49] T. Li, X. Liu, and H. Yu, "Backstepping nonsingular terminal sliding mode control for PMSM with finite-time disturbance observer," *IEEE Access*, vol. 9, pp. 135496–135507, 2021.
[50] X. Liu and H. Yu, "Continuous adaptive integral-type sliding mode control based on disturbance observer for PMSM drives," *Nonlinear Dyn.*, vol. 104, no. 2, pp. 1429–1441, Apr. 2021.
[51] M. Basin, "Finite- and fixed-time convergent algorithms: Design and convergence time estimation," *Annu. Rev. Control*, vol. 48, pp. 209–221, Jan. 2019.
[52] A. Polyakov, "Nonlinear feedback design for fixed-time stabilization of linear control systems," *IEEE Trans. Autom. Control*, vol. 57, no. 8, pp. 2106–2110, Aug. 2012.
[53] A. Polyakov and L. Fridman, "Stability notions and Lyapunov functions for sliding mode control systems," *J. Franklin Inst.*, vol. 351, no. 4, pp. 1831–1865, 2014.
[54] M. Basin, P. Yu, and Y. Shtessel, "Finite- and fixed-time differentiators utilising HOSM techniques," *IET Control Theory Appl.*, vol. 11, no. 8, pp. 1144–1152, May 2017, doi: 10.1049/iet-cta.2016.1256.
[55] M. V. Basin, P. Yu, and Y. B. Shtessel, "Hypersonic missile adaptive sliding mode control using finite-and fixed-time observers," *IEEE Trans. Ind. Electron.*, vol. 65, no. 1, pp. 930–941, Jan. 2018.
[56] J. Sun, J. Yi, Z. Pu, and X. Tan, "Fixed-time sliding mode disturbance observer-based nonsmooth backstepping control for hypersonic vehicles," *IEEE Trans. Syst., Man, Cybern., Syst.*, vol. 50, no. 11, pp. 4377–4386, Nov. 2020.
[57] B. Tian, Z. Zuo, X. Yan, and H. Wang, "A fixed-time output feedback control scheme for double integrator systems," *Automatica*, vol. 80, pp. 17–24, Jun. 2017.
[58] J. Zhang, S. Yu, and Y. Yan, "Fixed-time output feedback trajectory tracking control of marine surface vessels subject to unknown external disturbances and uncertainties," *ISA Trans.*, vol. 93, pp. 145–155, Oct. 2019, doi: 10.1016/j.isatra.2019.03.007.
[59] T. Wu, H. Wang, Y. Yu, Y. Liu, and J. Wu, "Quantized fixed-time fault-tolerant attitude control for hypersonic reentry vehicles," *Appl. Math. Model.*, vol. 98, pp. 143–160, Oct. 2021.
[60] J.-D. Lee, S. Khoo, and Z.-B. Wang, "DSP-based sliding-mode control for electromagnetic-levitation precise-position system," *IEEE Trans. Ind. Informat.*, vol. 9, no. 2, pp. 817–827, May 2013.
[61] M. Basin, Y. Shtessel, and F. Aldukali, "Continuous finite- and fixed-time high-order regulators," *J. Franklin Inst.*, vol. 353, no. 18, pp. 5001–5012, Dec. 2016.
[62] B. Su, H. Wang, and N. Li, "Event-triggered integral sliding mode fixed time control for trajectory tracking of autonomous underwater vehicle," *Trans. Inst. Meas. Control*, vol. 43, no. 15, pp. 3483–3496, Nov. 2021.
[63] Y. Pan, C. Yang, L. Pan, and H. Yu, "Integral sliding mode control: Performance, modification, and improvement," *IEEE Trans. Ind. Inf.*, vol. 14, no. 7, pp. 3087–3096, Jul. 2018.
[64] Z. Hou, P. Lu, and Z. Tu, "Nonsingular terminal sliding mode control for a quadrotor UAV with a total rotor failure," *Aerosp. Sci. Technol.*, vol. 98, Mar. 2020, Art. no. 105716.

ATUL SHARMA (Student Member, IEEE) received the B.E. degree in electrical engineering from the Department of Electrical Engineering, Samrat Ashok Technological Institute (SATI), Vidisha, India, in 2014, and the M.E. degree in digital techniques and instrumentation from the Department of Electrical Engineering, Shri G. S. Institute of Technology and Science (SGSITS), Indore, India, in 2017. He is currently pursuing the Ph.D. degree in control and automation with the Department of Electrical Engineering, Indian Institute of Technology Delhi, New Delhi, India. His research interests include control of nonlinear systems, robust control, sliding mode control, control of distributed parameter-based systems, embedded systems, renewable energy, and power electronics.

ABDULRAHMAN ALTURKI received the B.Sc. degree (Hons.) in electrical and communication engineering from Qassim University, Saudi Arabia, in 2008, and the M.Sc. and Ph.D. degrees in electrical engineering from the University of Dayton, OH, USA, in 2012 and 2017, respectively. He joined as an Assistant Professor with the Electrical Engineering Department, College of Engineering, Qassim University, in 2017. He has published several scientific papers in national and international conference proceedings and journals. His current research interests include computer vision, image restoration, multi-carrier communication systems, digital signal processing, digital communications, and channel equalization.

SYED MUHAMMAD AMRR (Graduate Student Member, IEEE) received the B.Tech. degree in electrical engineering and the M.Tech. degree in instrumentation and control from the Department of Electrical Engineering, Aligarh Muslim University (AMU), Aligarh, India, in 2014 and 2016, respectively, and the Ph.D. degree in control and automation from the Department of Electrical Engineering, Indian Institute of Technology Delhi (IITD), India, in 2021, where he is currently pursuing the Ph.D. degree. He has published more than 40 research papers in refereed international journals and conference proceedings. Furthermore, two international patents are also granted to his name, and he has authored a book chapter with CRC, Taylor and Francis, USA. His research interests include nonlinear control, sliding mode control, robust control, spacecraft systems, unmanned autonomous vehicles, constrained network control systems, renewable energy, and power electronics.